



## Supporting Online Material for

### **Kepler Planet-Detection Mission: Introduction and First Results**

William J. Borucki,\* David Koch, Gibor Basri, Natalie Batalha, Timothy Brown, Douglas Caldwell, John Caldwell, Jørgen Christensen-Dalsgaard, William D. Cochran, Edna DeVore, Edward W. Dunham, Andrea K. Dupree, Thomas N. Gautier III, John C. Geary, Ronald Gilliland, Alan Gould, Steve B. Howell, Jon M. Jenkins, Yoji Kondo, David W. Latham, Geoffrey W. Marcy, Søren Meibom, Hans Kjeldsen, Jack J. Lissauer, David G. Monet, David Morrison, Dimitar Sasselov, Jill Tarter, Alan Boss, Don Brownlee, Toby Owen, Derek Buzasi, David Charbonneau, Laurance Doyle, Jonathan Fortney, Eric B. Ford, Matthew J. Holman, Sara Seager, Jason H. Steffen, William F. Welsh, Jason Rowe, Howard Anderson, Lars Buchhave, David Ciardi, Lucianne Walkowicz, William Sherry, Elliott Horch, Howard Isaacson, Mark E. Everett, Debra Fischer, Guillermo Torres, John Asher Johnson, Michael Endl, Phillip MacQueen, Stephen T. Bryson, Jessie Dotson, Michael Haas, Jeffrey Kolodziejczak, Jeffrey Van Cleve, Hema Chandrasekaran, Joseph D. Twicken, Elisa V. Quintana, Bruce D. Clarke, Christopher Allen, Jie Li, Haley Wu, Peter Tenenbaum, Ekaterina Verner, Frederick Bruhweiler, Jason Barnes, Andrej Prsa

\*To whom correspondence should be addressed. E-mail: William.J.Borucki@nasa.gov

Published 5 January 2010 on *Science Express*  
DOI: 10.1126/science.1185402

#### **This PDF file includes:**

SOM Text  
Fig. S1  
References

**Correction:** The article title on the cover page has been edited to conform to *Science* style.

## SUPPORTING ONLINE MATERIAL

### TEXT

#### SOM 1. Instrument description

The instrument is a differential photometer with a wide (115 square degrees) field-of-view (FOV) that continuously and simultaneously monitors the brightness of approximately 150,000 main-sequence stars. The instrument is designed for a useful range of visual magnitudes ranging from 9 to 15. Although saturation occurs for stars brighter than  $m_v=11.5$ , measurements show excellent photometric performance from magnitude 7 through 17 (*S1*) when the photometric aperture is sufficiently large to measure the overflow. The photometer is based on a modified Schmidt telescope design that includes field flattening lenses near the focal plane that accommodate the flat detectors on the curved focal surface associated with the large FOV. The photometer uses a corrector with a 0.95 m aperture and a 1.4 m diameter f/1 primary. The 0.95 m aperture is sufficient to reduce the Poisson noise to the level required to obtain a  $4\sigma$  detection for a single transit from an Earth-size planet passing in front of a  $V=12^{\text{th}}$  magnitude G2 dwarf (i.e., Sun-like stars) with a 6.5 hour transit. The focal plane is composed of forty-two 1024x2200 backside-illuminated CCDs with 27  $\mu\text{m}$  pixels. The 5% band pass wavelengths are 423 nm and 897 nm.

Two cadences are available for data acquisition;  $\sim 1$  minute and  $\sim 30$  minutes which are summed onboard the spacecraft from 6.02 second exposures. A maximum of 170,000 targets can be accommodated at the 30 minute cadence and 512 at the 1 minute cadence. The shorter cadence is used for high resolution measurements needed for transit timing variations, eclipsing binary timing, and for asteroseismology.

#### SOM 2. Target Selection

To remove the many giant stars in our FOV from the target list, a 5 year program of ground based multi-band photometric observations of  $6 \times 10^6$  stars in the FOV classified each star. The results were assembled into the *Kepler Input Catalog (KIC)* that is now available to the public. This catalog provides the effective temperature and surface gravity which can be combined to estimate the size of the star and to distinguish dwarfs from giant stars. The target stars are chosen from the  $4.5 \times 10^6$  stars that are imaged onto active silicon of the detector array (*S2*). Most giant stars are avoided, as the stellar size and variability make it much more difficult to detect small planets. On average, only about 38 pixels for each star are sent to the ground where the photometry is done. (*S2*)

#### SOM 3. Identification of False Positive Events

To accurately determine the frequency of planets, *Kepler* must identify false-positive events; i.e., transit-like signals that are not caused by a transiting planet. There are two general types of false positive events; statistical or systematic fluctuations in the time series and astrophysical phenomena that produce similar signals. The *Kepler* pipeline applies a series of tests to avoid statistical false positives (*S3*, *S4*). Rejecting astrophysical false positives requires a combination of *Kepler* data and observations from the *Kepler* Follow-up Observation Program. (*S5*).

The *Kepler* data-processing pipeline reduces the photometric observations of each star and searches each time series for threshold crossing events (TCE), a pattern of transits that exceed a  $7.1\text{-}\sigma$  threshold (*S6*) and might be caused by a planetary transit. The TCE then undergo a series of tests to determine if some astrophysical process is present such as a small star orbiting the target star, or an eclipsing binary is present in the aperture, or there is a third star that is diluting the amplitude of the transit.

To identify stellar companions and background false-positive objects and to measure the masses of the planets; radial velocity, active optics, and speckle observations were conducted at the Keck I, Hobby-Eberly, Harlan J. Smith 2.7m, Hale, WIYN, MMT, Tillinghast, Shane, and Nordic Optical Telescopes. Similar to the results of the CoRoT Mission, many events were found to be false positives (*S5*); usually background eclipsing binaries (*S7*).

#### SOM 4. Determination of the Characteristics of Discovered Planets

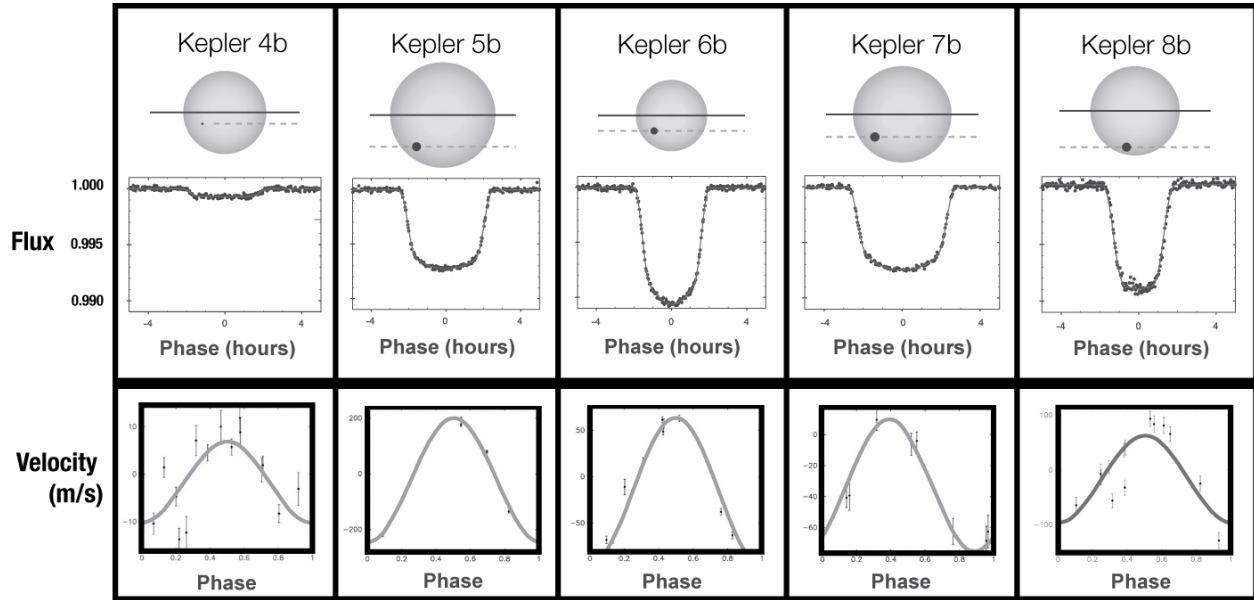
Once a planet has been identified, the semi-major axis can be derived using Kepler's 3<sup>rd</sup> Law, the orbital period from *Kepler* photometry, the mass of the host star. There is a weak dependence on planet mass, but this is rarely substantial and can be accounted for when radial velocity (RV) observations measure the planet mass. The planet's equilibrium temperature can be estimated from the size of the star, its effective temperature, and its semi-major axis. Formally, the equilibrium temperature also depends on the orbital eccentricity and the albedo, but these are modest effects except for large eccentricities and high albedos. If this temperature is consistent with the possibility of liquid water on the surface of the planet, then the planet is deemed to be in the habitable zone; i.e. in a temperature regime favorable to the evolution of life. Of course, a planet's actual surface temperature also depends on the greenhouse factor which is a function of the mass of the planet and the properties of its atmosphere.

The ratio of the planet area to the star area can be directly measured from the transit depth (after accounting for dilution by starlight from nearby stars, the orbital inclination, and limb darkening effects). Therefore it is critical to estimate the sizes of the stars hosting planets. If the orbital eccentricity of the planetary orbit is known, then precise measurements of the transit duration and orbital period provide an excellent determination of the mean stellar density (*S8*, *S9*). When combined with spectroscopic measurements and stellar modeling, the stellar size and mass can be determined. While RV observations and/or measurements of the occultation can be used to measure the eccentricity, it is important to have independent measurements of the stellar size. Asteroseismology analysis is being used to determine the mean stellar density and to estimate the size, mass, and age of target stars. Then these parameters are used to derive the size and age of the planets.

Although asteroseismic analysis of the optical flux variations of bright target stars provide the best estimate of stellar size, other methods are needed for the large number of dimmer stars. Astrometry on the image centroids can measure the parallax and thus distance to the star (*S10*). When this distance is combined with photometric measurements (e.g., those from KIC), spectroscopic observations and stellar modeling, one can estimate the stellar luminosity, temperature, size and mass.

## FIGURES AND LEGEND

SOM 5. Light curves and RV observations of the first planets detected by *Kepler*.



**S1. Light curves and RV observations of the first planets detected by *Kepler*.** All parameters, such as stellar size, depth and duration of transit, and impact parameter use the same relative scale.

### References:

- S1. Gilliland, R.L., et al., Initial Characteristics of *Kepler* Short Cadence Data. *Astrophys. J.* astro-ph 1001.0142 (2010).
- S2. Batalha, N. et al., Selection, prioritization, and characterization of *Kepler* target star. *Astrophys J.*, astro-ph 1001.0349 (2010).
- S3. Batalha, N. et al., Pre-spectroscopic false positive elimination of *Kepler* planet candidates., *Astrophys. J.*, submitted.
- S4. Jenkins et al., 2009b, Overview of the *Kepler* Science Operations Center processing pipeline. *Astrophys. J.*, submitted.
- S5. Gautier, T.N. et al. *Astrophys. J.*, submitted
- S6. Jenkins, J.M., *Astrophys. J.* **575**, 493 (2002).
- S7. Almenara, J.M., H.J. Deeg, S Aigrain, R. Alonso, M. Auvergne, A. Baglin et al. *Astron. Astrophys.* **506**, 337 (2009).
- S8. Seager, S., G. Mallen-Ornelas. *Astrophys. J.*, **585**, 1038 (2003)
- S9. Sozzetti, A., G. Torres, D. Charbonneau, D. W. Latham, M. J. Holman, J. Torres, G. *Astrophys. J.* **671** L65 (2007).
- S10. Monet, D., et al. *Astrophys. J.* submitted